on degree angular scales or multipoles of $\ell \sim 80$, typically referred to as the recombination peak, and another contribution for multipoles of $\ell \lesssim 10$ from the epoch of reionization.

No sub-orbital experiment has yet measured modes at $\ell < 40$. The temporal stability, absence of atmospheric noise, and full-sky coverage offered by a satellite like PICO make it the most suitable instrument to reach these lowest multipoles.

The contribution from reionization is expected to be strongest relative to the contributions from instrumental noise and "lensing" B-modes created from E-modes by the deflection of photons by large-scale structure on their way to us from the last-scattering surface.

When the tensor-to-scalar ratio $r \simeq 0.01$, the BB lensing power spectrum and the primordial BB power spectrum are comparable around the recombination peak. For lower levels of r, the lensing B-modes dominate, but the B-mode maps can be "delensed" [23, 24]. The effect of lensing on E and B maps can be determined and undone if these maps are measured with few-arcmin resolution and sufficient depth. Forecasts for PICO show that at least 73% of the lensing B-mode power can be removed for the baseline configuration, after accounting for foreground subtraction, 80% will be removed if the foregrounds do not degrade the inherent SNR significantly, rising to 85% for the CBE configuration. Delensing will improve PICO's determination of r by a factor of 4–6. We emphasize that PICO will be relying on its own data to conduct the delensing and foreground cleaning, thus avoiding reduced efficacy arising from the need to cross-calibrate experiments, identify common observing areas on the sky, not having frequency-band coverage at the appropriate resolution to remove foregrounds, or from other systematic uncertainties.

Models of the early universe differ in their predictions for the scalar spectral index n_s and its scale dependence, often referred to as the running of the spectral index n_{run}. With its high resolution and low noise levels, PICO will improve the constraints on n_s and n_{run} by a factor of about two. In addition, PICO will probe the statistical properties of the primordial fluctuations over a wide range of scales with exquisite precision and improve constraints on departures from Gaussianity by a factor of 2–3. By cross-correlating the lensing map with large-scale structure data from LSST it may even be possible to reach a theoretically important threshold (see, e.g. [25] and references therein) and constrain local non-Gaussianity to better than $\sigma(f_{NL}) = 1$. This is discussed in more detail in section 2.2.2.

Fundamental Particles: Light relics, Dark Matter, and Neutrinos

• **Light Relics** In the inflationary paradigm, the universe was reheated to temperatures of at least 10 MeV and perhaps as high as 10^{12} GeV. At these high temperatures, even very weakly interacting or very massive particles, such as those arising in extensions of the Standard Model of particle physics, can be produced in large abundances [26, 27]. As the universe expands and cools, the particles fall out of equilibrium, leaving observable signatures in the CMB power spectra. Through these effects the CMB is a sensitive probe of neutrino and of other particles' properties.

One particularly compelling target is the effective number of light relic particle species N_{eff}. The canonical value with three neutrino families is $N_{eff} = 3.046$. Additional light particles contribute a universal change to N_{eff} that is a function only of the decoupling temperature and the effective degrees of freedom of the particle, g. Furthermore, the range of ΔN_{eff} is quite restricted, even for widely varying decoupling temperatures T_F, with the range $0.027\,g \leq \Delta N_{eff} \leq 0.07\,g$ corresponding to decoupling at higher temperatures during post-inflation reheating ($0.027g$) to lower temperatures shortly prior to the QCD phase transition ($0.07g$).

Performance forecasts for N_{eff} are shown in Figure 3. For an experiment like PICO, which has

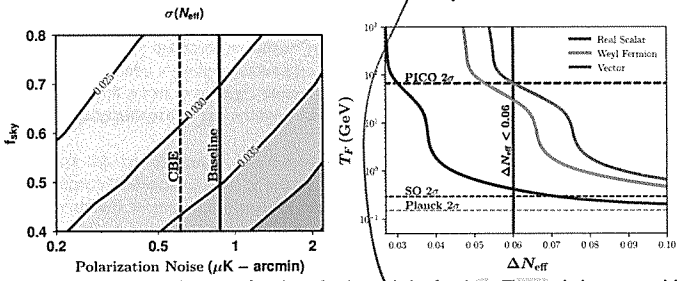

Figure 3: *Left:* N_{eff} uncertainty as a function of noise and sky fraction. The resolution assumed is 5'. Vertical lines denote the expected performance of the baseline mission. *Right:* Reach in the freeze-out temperature for various species, given a measurement of ΔN_{eff}. We see an exclusion of $\Delta N_{eff} < 0.06$ is a nearly two-orders-of-magnitude improvement over Planck and SO. The vertical lines are normalized to the T_F for a single vector particle.

sufficient resolution to reach cosmic-variance-limited measurement of EE up to $\ell = 2300$, the two additional most important parameters for improving constraints are the fraction of sky observed f_{sky} and the noise. Achieving both larger f_{sky} and lower noise are strengths of PICO compared to other platforms. The PICO requirement is to constrain $\Delta N_{eff} < 0.06$ at 95%. The corresponding improvement in reach in T_F is shown in the right panel of Figure 3. The large improvement over Planck ($\Delta N_{eff} < 0.28$, 95%) corresponds to a factor of 400 improvement in the limit on the decoupling temperature for any particle with spin.

Many light relics of the early universe are not stable. They decay, leaving faint evidence of their past existence on other tracers. The relics with sufficiently long lifetime to survive few minutes, past the epoch of light-element synthesis, leave a signature on the helium fraction Y_P. If they decay by the time of recombination, their existence through this period is best measured through the ratio of N_{eff} to Y_P. At both CBE and Baseline sensitivity, PICO can simultaneously measure N_{eff} and Y_P with $\sigma(N_{eff}) = 0.08$ and $\sigma(Y_P) = 0.005$. Alternatively, PICO can measure Y_P at fixed N_{eff} with $\sigma(Y_P) = 0.002$ to independently determine the primordial helium abundance with the same precision as astrophysical measurements. The combination of these measurements is a sensitive test of physics between big-bang nucleosynthesis and recombination.

• **Dark Matter** Cosmological measurements have already confirmed the existence of one relic that lies beyond the Standard Model: dark matter. For a conventional WIMP candidate, the CMB places very stringent constraints on its properties through the signature of its annihilation [28–30]. Most of this information is in the EE power spectrum at $50 < \ell < 300$, and is well-measured by *Planck* and will approach the cosmic-variance limit with existing ground-based surveys [31, 32]. An entirely complementary way to probe dark matter is to search for evidence of its interactions with other species in cosmological data. Since a lower mass translates to a higher number density of scattering centers, CMB is particularly sensitive to the low-mass regime and is sensitive to large, nuclear-scale cross-sections.

Interactions between dark matter and protons in the early universe creates a drag force between the two cosmological fluids, damping acoustic oscillations and suppressing power in density per-

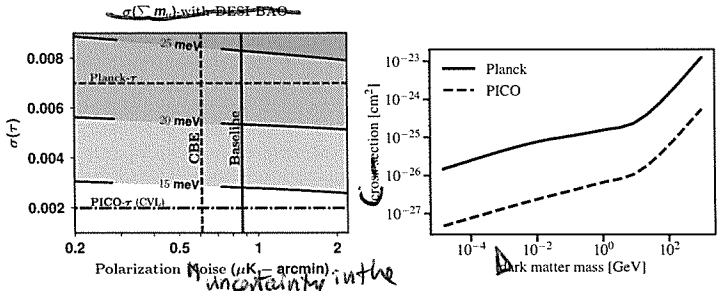

Figure 4: *Left:* Forecasts for the sum of neutrino masses uncertainty, including DESI BAO, as a function of noise and the uncertainty in the measurement of τ, for 0.7 sky fraction. The upper blue dashed line is the current *Planck* limit; the lower grey dashed line is the limit from cosmic-variance-limited measurement of τ. *Right:* Upper limits on DM-proton interaction cross-section as a function of DM mass, for a spin-independent velocity-independent scattering. Areas above the curves are excluded at 95% confidence-level. Shown are the current limits from *Planck* [36]) and a forecast for PICO.

turbations on small scales. As a result, the CMB temperature, polarization, and lensing power spectra are suppressed at high multipoles relative to a universe without such drag forces. This effect has been used to search for evidence of dark matter-proton scattering over a range of masses and couplings, and to provide consistency tests of dark matter in the context of the anomalous 21-cm signal reported by the EDGES collaboration [33–41]

In Figure 4, we present current and projected upper limits on the dark matter-proton interaction cross-section as a function of dark matter mass, for a spin-independent velocity-independent scattering (chosen as our fiducial model). Regions above the curves are excluded at the 95% confidence level. We compare current limits obtained from *Planck* (from [36]) with projections for PICO sensitivity. We note that PICO can deliver a substantial improvement over the current limits, across the entire dark-matter mass range considered. Most of the constraining power in case of PICO (and ground-based next-generation measurements with similar white-noise levels) comes from the measurement of the lensing power spectrum.

• **Neutrino Mass** The origin and structure of the neutrino masses is one of the great outstanding questions about the nature of the Standard Model particles. Measurements of neutrinos in the lab have revealed much about the mass differences and mixing angles. Cosmology offers a measurement of the sum of the neutrino masses $\sum m_\nu$ through the gravitational influence of the non-relativistic cosmic neutrinos. The measurement of $N_{\rm eff} = 2.99 \pm 0.17$ [42] already confirms the existence of these neutrinos at $> 10\sigma$ and their mass implies that they will contribute to the matter density at low redshifts. The best current mass constraint arises from a combination of Planck and BOSS baryon acoustic oscillations (BAO) giving $\sum m_\nu < 0.12$ eV (95%) [42].

Cosmological measurements are primarily sensitive to the suppression of power on small scales after the neutrinos become non-relativistic, which can be measured via CMB lensing or weak lensing in a galaxy survey. However, these measurements are limited by our knowledge of the amplitude of the primordial fluctuation power spectrum, A_s. In practice, CMB observations most

directly constrain $A_s e^{-2\tau}$ and thus do not provide a high-precision measurement of either A_s or τ separately.

Although many surveys hope to detect $\sum m_\nu$, any detection of the minimum value expected from particle physics, $\sum m_\nu = 58$ meV, at more than 2σ will require a better measurement of τ. The best constraints on τ come from E modes with $\ell < 20$, which require measurements over the largest angular scales. To date, the only proven method for such a measurement is from space. The current limit of $\sigma(\tau) = 0.007$ is from *Planck* [43]. Forecasts for a CMB measurement of $\sum m_\nu$ using the lensing B modes [44] are shown in Figure 3. With the current uncertainty in τ one is limited to $\sigma(\sum m_\nu) \gtrsim 25$ meV (including DESI BAO); no other survey or cosmological probe would improve this constraint. But PICO will reach the cosmic-variance limit of $\tau \sim 0.002$ and will therefore reach $\sigma(\sum m_\nu) < 15$ meV when combined with DESI's measurements of baryon acoustic oscillations [45]. Robustly detecting neutrino mass at $> 3\sigma$ in any cosmological setting is only possible with an improved measurement of τ like the one achievable with PICO. This measurement would give $\sum m_\nu > 0$ at greater than 4σ or would exclude the inverted hierarchy ($\sum m_\nu > 100$ meV) at 95% confidence, depending on the central value of the measurement. Lab-based measurement could determine the hierarchy before PICO, but only cosmology can measure $\sum m_\nu$.

Fundamental Fields: Primordial Magnetic Fields and Cosmic Birefringence

• **Primordial Magnetic Fields** One of the long-standing puzzles in astrophysics is the origin of 1–10 μG strength galactic magnetic fields [46]. Producing such fields through a dynamo mechanism would require a primordial seed field [47]. Moreover, μG-strength fields have been observed in proto-galaxies that are too young to have gone through the number of revolutions necessary for the dynamo to work. A primordial magnetic field (PMF), present at the time of galaxy formation, could provide the seed or even eliminate the need for the dynamo altogether. Specifically, a $\gtrsim 0.1$ nG field in the intergalactic plasma would be adiabatically compressed in the collapse to form a $\gtrsim 1$ μG galactic field [48]. PMFs could have been generated in the aftermath of phase transitions in the early universe [49], during inflation [50, 51], or at the end of inflation [52]. A detection of PMFs would be a major discovery, signalling physics beyond standard models of particle physics and cosmology, and constraints on PMFs offer a valuable tool for discriminating among different theories of the early universe [53–55]. While the PMF would be sustained by the primordial plasma well beyond recombination, with signatures at low redshifts, only seeing them in CMB would conclusively prove their primordial, as opposed to an astrophysical, origin.

The signature of PMFs is detectable through Faraday rotation [56], which converts E modes into B modes, and through generating signatures in the BB power spectrum at high ℓ [57]. The current CMB bounds on PMF strength are $B_{1\rm Mpc} < 1.2$ nG at 95% CL for the scale-invariant PMF spectrum [58]. PICO's sensitivity and resolution would allow to probe PMFs as weak as 0.1 nG (1σ), a limit that already includes the effects of imperfect lensing subtraction, galactic foregrounds [59–61], and other systematic effects. It would, nevertheless, be an important improvement that will conclusively rule out the purely primordial (no dynamo) origin of the largest galactic magnetic fields.

• **Cosmic Birefringence** The simplest model for late-time acceleration of the universe is with a slowly-evolving scalar field, the quintessence [62]. Such a field generically couples to electromagnetism through a Chern-Simons-like term, and causes linear polarization of photons propagating cosmological distances to rotate. This is known as cosmic birefringence [62]. The birefringence converts primordial E mode into B mode. It thus produces parity-violating TB and EB

cross-correlations whose magnitude depends on the statistical properties of the rotation field in the sky [63, 64]. There are no theoretical predictions for the level of birefringence, but if observed, it would be evidence for physics beyond the standard model and a potential probe of dark-energy microphysics [64–66]. Using the sensitivity of only the 155 GHz, PICO will improve current constraints on cosmic birefringence (from POLARBEAR [67]) by a factor of 300. The constraints will be even stronger when including all frequency bands.

2.2.2 Cosmic Structure Formation and Evolution

The Formation of the First Luminous Sources The reionization of the Universe imprints multiple signals in the temperature and polarization of the CMB. In polarization, the most important signal is an enhancement in the EE power spectrum at large angular scales $\ell \lesssim 20$ (see Figure 1). This signal gives a direct measurement of the optical depth to the reionization epoch τ, and thus to the mean redshift of reionization z_{re} with very little degeneracy with other cosmological parameters (see Figure 5). The mean redshift of reionization z_{re} (when 50% of the cosmic volume was reionized) depends sensitively on the nature of the ionizing sources. It is currently unknown whether star-forming galaxies or more exotic sources such as supermassive black holes drove the reionization process. What was the mean free path of ionizing photons during this epoch? What was the efficiency with which such photons were produced by ionizing sources? What were the masses and environments of the dark-matter halos that hosted the sources? These properties all affect z_{re}. Furthermore, the detailed shape of the low-ℓ E-mode power spectrum is sensitive to the reionization history itself (i.e., $d\tau/dz$), and will provide information beyond that captured in τ alone. For example, it has been argued that *Planck* data show evidence for an extended tail of reionization out to $z \approx 15$–20 [68]. A cosmic-variance-limited measurement of the large-scale E modes, as obtained by PICO, will settle this question.

Large-scale EE power spectrum measurements are a unique and crucial observable for many aspects of cosmology, particularly the growth of structure. If measurements of τ are not improved beyond the current uncertainties from *Planck*, inference of several new signals of cosmological physics will be severely hindered. A canonical example is the inference of the sum of the neutrino mass (see page 10), but any cosmological inference related to the growth of structure will be affected to some extent, including constraints on dark energy and modified gravity from weak lensing, cluster counts, and similar structure probes. PICO is the ideal experiment to resolve this issue. Its noise level and frequency coverage permit a cosmic-variance-limited constraint on τ, i.e., $\sigma(\tau) \approx 0.002$, which we have verified with explicit forecasts including separation of foregrounds.

In temperature, an important imprint of reionization is that sourced at small angular scales by the "patchy" kinematic Sunyaev-Zel'dovich (kSZ) effect, due to the peculiar velocities of free electron bubbles around ionizing sources. Measurements of the small- scale kSZ power spectrum, with instruments that have higher resolution than PICO, can give constraints on the duration of reionizaiton Δz_{re} [69]. Fig. 5 presents forecasts for reionization constraints in the $z_{re} - \Delta z_{re}$ parameter space obtained from PICO's measurement of τ in combination with ground-based Stage-III CMB experiments measurements of the kSZ power spectrum. The PICO measurement of τ is essential for breaking degeneracies and allowing simultaneous, precise constraints to be placed on both the mean redshift and duration of reionization. The figure also shows curves of constant efficiency of production of ionizing photons in the sources, and of intergalactic-medium opacity. These are two parameters that quantify models of reionization. The curves shown are illustrative; families of models, that would be represented by parallel 'source efficiency' and 'IGM Opacity' lines, are

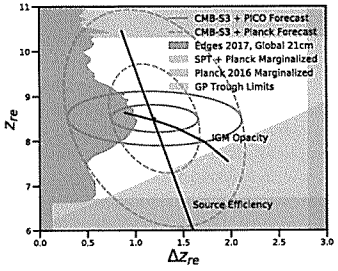

Figure 5: Contours of 1 and 2σ constraints on the mean redshift and duration of reionization using PICO and CMB-S3 data (solid dark blue), and comparison with *Planck* and CMB-S3 (dashed light blue). Source efficiency and IGM opacity (dark lines) are two physical parameters controlling the reionization process in current models. The PICO measurements together with higher resolution data of the kSZ effect will significantly the range of models allowed. We also include other constraints from *Planck*, EDGES, the Gunn-Peterson (GP) trough, and *Planck*+ the South Pole Telescope (SPT) [42, 70–72].

allowed by current data. PICO's data will give simultaneous constraints on these physical parameters, yielding important information on the nature of the first luminous sources. For example, galaxies or quasars predict significantly different values for these parameters.

In addition to these signals, reionization also leaves specific non-Gaussian signatures in the CMB. In particular, patchy reionization induces non-trivial 4-point functions in both temperature [73] and polarization [74]. The temperature 4-point function can be used to separate reionization and late-time kSZ contributions. Combinations of temperature and polarization data can be used to build quadratic estimators for reconstruction of the patchy τ field, analogous to CMB lensing reconstruction. These estimators generally require high angular resolution, but also rely on foreground-cleaned CMB maps. Thus, while PICO alone may not enable high SNR reconstructions, its high-frequency bands — which have better than 2 arcmin resolution and cover frequencies that are not suitable for observations from the ground — will enable these estimators to be robustly applied to ground-based CMB data sets, a strong example of ground-space complementarity.

Structure Formation via Gravitational Lensing Matter between us and the last-scattering surface deflects the path of photons through gravitational lensing, imprinting the 3-dimensional matter distribution across the volume of the Universe onto the CMB maps. The specific quantity being mapped by the data is the projected gravitational potential ϕ that is lensing the photons. From the lensing map, which receives contributions from all redshifts between us and the CMB with the peak of the distribution at $z \simeq 2$, we infer the angular power spectrum $C_L^{\phi\phi}$.[3] Both the temperature and polarization maps of the CMB, and by extension the angular power spectra, are affected by lensing.

Planck's ϕ map had SNR of $\sim$1 per L mode over a narrow range of scales, $30 < L < 50$. PICO's map would represents true mapping, with SNR > 1 per each mode down to scales of approximately ten arcminutes ($L \sim 1000$); see Figure 6. On smaller scales, the map will still contain statistical information. While *Planck* had an SNR of 40 integrated across the $C_L^{\phi\phi}$ power spectrum [75], the PICO combination of resolution, sensitivity, and sky coverage enables a measurement with SNR of 640 and 740 for the baseline and CBE configurations, respectively. When accounting for possible foreground contamination, its broad frequency coverage leads to a reduction of SNR of less than 20% (see Figure 6).

[3] We use L to refer to multipoles in the CMB lensing and galaxy clustering fields, in contrast to the use of ℓ for the CMB itself; this is because of the different geometry — a range of ℓ corresponds to each L in the 4-point function.

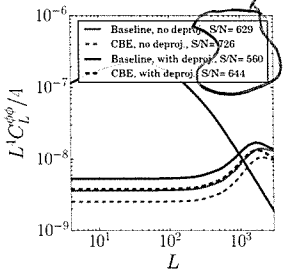

Figure 6: Theoretically predicted lensing power spectrum $C_L^{\phi\phi}$ (black) and forecasted PICO noise levels, with (red), and without (blue) deprojection, that is i.e., removal, of foregrounds. PICO will make a map of ϕ at angular scales where the noise is below the signal.

The value of the reconstructed lensing map is immense, as has already been demonstrated with the much lower SNR map from *Planck*. The unprecedented constraints on neutrino mass, discussed on page 10, are a direct result of this deep map. Tomographic cross-correlations of the lensing map with samples of galaxies and quasars will yield constraints on structure formation. The measurements will constrain the properties of quasars and other high-redshift astrophysics, e.g., a precise determination of the quasar bias (and hence host halo mass) as a function of their properties, such as (non-)obscuration. The map will be cross-correlated with other large-scale tracers to probe fundamental physics. For instance, one can use correlations between large-scale structure tracers with different clustering bias factors to effectively cancel cosmic variance [76, 77] and constrain physics that affects the biasing of objects on large scales, such as primordial local non-Gaussianity [78]. In Fig. 7 we show the expected constraints for the CMB lensing field as reconstructed with PICO, in cross-correlation with three years of the LSST survey. It can be seen that depending on the minimal multipole that can be used in the cross-correlation, which is uncertain in both LSST and the PICO lensing map, the well-motivated theory target of $\sigma(f_{\rm NL}) \simeq 1$ [25] can be within reach. Values of $f_{\rm NL}$ at or above this level are a generic prediction of multi-field inflationary models.

Using the same cross-correlation techniques, it is also possible to constrain the evolution of the amplitude of structure as a function of redshift. Figure 8 shows constraints on the amplitude of linear structure in several redshift bins. This is a model-independent representation of the structure growth constraints; these measurements will yield constraints on dark energy or modified gravity, in the context of specific models. The measurements can also be used for a neutrino mass constraint that is complementary to and competitive with that inferred from the CMB lensing auto-power spectrum described earlier.

Lensing will also be used to weigh dark matter halos hosting galaxies, groups, and clusters of galaxies. Calibrating the masses of galaxy clusters is the most uncertain and crucial step in the cluster cosmology program, in which CMB lensing has already begun to play an important role. In this approach, known as CMB halo lensing, we focus on the small-scale effects of gravitational lensing around these objects [79–81]. The technique holds great potential for measuring halo masses out to high redshifts where gravitational lensing of galaxies (i.e., gravitational shear) no longer works because of the lack of background sources.

This is illustrated in Fig. 9, which shows the mass sensitivity of PICO using a spatial filter optimized for extracting the mass of halos [82]. The curves give the one-sigma noise in a mass

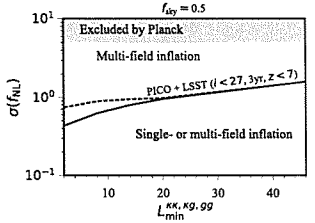

Figure 7: Forecasted sensitivity to the parameter describing primordial non-Gaussianity of the local type for the PICO CMB lensing map together with three years of the LSST survey, as a function of the minimal multipole used in the analysis. A value of $\sigma(f_{\rm NL}) \simeq 1$ is a well-motivated theoretical target.

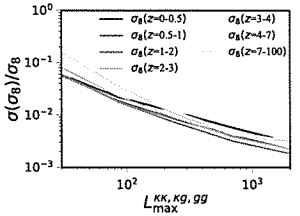

Figure 8: Forecasted sensitivity to the parameter describing the amplitude of structure in various redshift bins, as a function of the maximal multipole used in the analysis. Percent-level constraints on these parameters allow for stringent tests of physics beyond ΛCDM that modify the rate of growth of structure.

measurement through the filter as a function of redshift. Their flattening at high redshift reflects the fact that CMB lensing is sensitive over a broad range of redshifts, extending well beyond the limit of $z = 2$ of the figure. We see that PICO can measure the mass of individual low-mass clusters ($\sim 10^{14}\,{\rm M}_\odot$) over a wide redshift range, and by stacking we can determine the mean mass of much smaller halos, including those hosting individual galaxies.

Halo lensing will enable calibration of the galaxy cluster mass scale, which is critical for our cosmological analysis of PICO cluster counts, as mentioned above. It also gives a unique tool for measuring the relation between galaxies and their dark matter halos during the key epochs of cosmic star formation at $z \geq 2$, not reachable by other means. This will provide valuable insight into the role of environment on galaxy formation during the rise to and fall from the peak of cosmic star formation at $z \sim 2$. From a complementarity perspective, the high-resolution, high-frequency PICO channels will play an essential role in cleaning foregrounds for high-resolution ground-based halo-lensing measurements at lower frequencies, particularly those derived from the temperature-based estimator, which is most contaminated by foregrounds.

Galaxy Formation via the Sunyaev-Zel'dovich (SZ) Effects Not all CMB photons propagate through the Universe freely; about 6% are Thomson-scattered by free electrons in the intergalactic medium (IGM) and intracluster medium (ICM). These scattering events leave a measurable imprint on CMB temperature fluctuations, which thereby contain a wealth of information about the growth of structures and the thermodynamic history of baryons. A fraction of these photons are responsible for the thermal and kinetic Sunyaev–Zel'dovich effects (tSZ and kSZ) [83, 84]. The amplitudes of the tSZ and kSZ signals are proportional to the integrated electron pressure and momentum along the line of sight, respectively. They thus contain information about the thermodynamic properties of the IGM and ICM, which are highly sensitive to astrophysical 'feedback'. Feedback is the process of energy injection into the IGM and ICM from accreting supermassive black holes, supernovae, stellar winds, and other sources. The tSZ effect will be used to measure ensemble

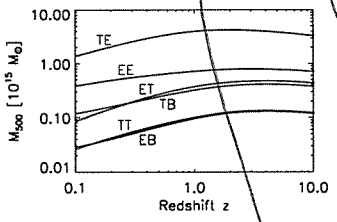

Figure 9: PICO sensitivity for CMB halo lensing. Curves for different CMB signal correlations give the one-sigma sensitivity of an optimal mass filter [82]. The curves are flat at high redshift, demonstrating the essential property that CMB halo lensing can be applied over a very wide redshift range, and well beyond the $z = 2$ limit of the figure. For PICO, the EB and TT estimators are roughly equivalent, offering important cross-validation of measurements because the systematics are very different for temperature and polarization.

statistics of galaxy clusters, which contain cosmological information, as well as to provide uniform cluster samples for galaxy formation studies in dense environments.

• **Galaxy Clusters** Galaxy clusters found via the tSZ effect provide a well-defined sample with a simple-to-model selection function. Samples of clusters such as these are straightforward to use for cosmological inference and studies of galaxy evolution in dense environments. The tSZ-selected sample from PICO will provide all clusters with masses above $\sim 3 \times 10^{14} M_\odot$ (defined with respect to the radius within which the average density reaches 200 times the critical) out to high redshifts, as long as the clusters have started to virialize. We forecast that PICO will find $\sim$150,000 galaxy clusters, assuming the cosmological parameters from *Planck* and applying a galaxy mask, using only 70% of the sky. With redshifts provided by optical surveys and infrared follow-up observations, the PICO tSZ-selected cluster sample will be an excellent cosmological probe, with mass calibration provided by CMB halo lensing described above and optical weak lensing for clusters with $z < 1.5$.

• **Compton-y map and tSZ auto-power spectrum** In addition to finding individual clusters, multifrequency CMB data also allow the reconstruction of full-sky maps of the tSZ signal. These are called 'Compton-y maps'. With its extremely low noise and broad frequency coverage, which is essential for separating out other signals, PICO will yield a definitive Compton-y map over the full sky, with high SNR down to angular scales of a few arcminutes. We quantify this expectation by reconstructing the Compton-y field using the needlet internal linear combination (NILC) algorithm [85] applied to sky simulations generated with the *Planck* sky model, with maps at all PICO frequencies (with appropriate noise added). The error bars on the reconstructed tSZ power spectrum are shown in Fig. 10, in comparison to current measurements. The total SNR is 1270 for the PICO CBE configuration, with the PICO baseline configuration only $\sim$10% lower. This is nearly two orders of magnitude higher SNR compared to *Planck*, which has already provided data with much higher SNR compared to ground-based experiments.

Extremely strong constraints on models of astrophysical feedback will be obtained from the analysis of the PICO y-map, both from its auto-power spectrum and from cross-correlations with galaxy, group, cluster, and quasar samples. Like the CMB-lensing map described above, the legacy value of the PICO y-map will be immense. As an example, we forecast the detection of cross-correlations between the PICO y-map and galaxy weak lensing maps constructed from LSST and WFIRST data. Considering the LSST "gold" sample with a source density of 26 galaxies/arcmin^2 covering 40% of the sky, we forecast a detection of the tSZ–weak lensing cross-correlation with S/N = 3000. At this immense significance, the signal can be broken down into dozens of tomographic redshift bins, yielding a precise breakdown of the evolution of thermal pressure over

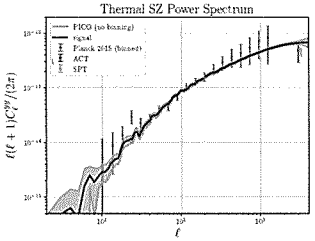

Figure 10: Constraints on the tSZ power spectrum from PICO and current data. A simulated tSZ power spectrum (black) is constrained at each multipole by PICO's data (1σ, green). Binning in ℓ, would increase the SNR beyond the calculated value of 1270, which is already nearly 100 times larger than *Planck* (blue). We include current measurements by SPT and ACT, and ground-based programs [86, 87].

cosmic time. For PICO and WFIRST (assuming 45 galaxies/arcmin^2 covering 5.3% of the sky), we forecast S/N = 1100 for the tSZ–weak lensing cross-correlation. The WFIRST galaxy sample extends to higher redshift, and thus this high S/N measurement will allow the evolution of the thermal gas pressure to be probed to $z \approx 2$ and beyond (the peak of the cosmic star-formation history). These transformative measurements will revolutionize our understanding of galaxy formation and evolution by distinguishing between models of feedback energy injection at high significance. Additional cross-correlations of the PICO y-map with quasar samples, filament catalogs, and other large-scale structure tracers will further demonstrate its immense legacy value, providing valuable information on baryonic physics that is complementary to inferences from the lensing cross-correlations described earlier.

2.2.3 Galactic Structure and Star Formation

Observations of Galactic polarization are a highlight and a lasting legacy of the *Planck* space mission. Spectacular images combining the intensity of dust with the texture derived from polarization data have received world-wide attention and have become part of the general scientific culture [88]. Beyond their popular impact, the Planck polarization maps represented an immense step forward for Galactic astrophysics [89]. We expect an even greater leap forward from PICO, based on the higher angular resolution dust polarization images obtained with the balloon experiment BLAST-Pol. PICO will provide all-sky maps of dust polarization at higher resolution than BLASTPol and with significantly higher sensitivity than *Planck* (See Figure 11.) Such a data set can only be obtained from a space mission. The data will complement a rich array of polarization observations, including stellar polarization surveys, to be combined with Gaia astrometry and synchrotron observations measuring Faraday rotation at radio wavelengths with the Square Kilometer Array and its precursors. Here, we focus on two key crucial Galactic science measurements that require PICO.

(1) *Testing Composition Models of Interstellar Dust:* PICO will enable spectral characterization of Galactic polarization. This in turn enables us to refine and test models of dust composition and grain alignment, which are of interest for the interpretation of dust polarization data at large.

(2) *Determining how magnetic fields affect the processes of molecular cloud and star formation:* By virtue of the strong dynamical coupling of dust and gas and the systematic alignment of dust grains with magnetic fields, dust polarization probes magnetic fields in the cold and warm neutral phases of the diffuse ISM (which contains the bulk of the ISM gas mass and turbulent energy) down to the scale of molecular clouds (which are where stars form). PICO will measure polarization across this broad range of scales to trace the role of magnetic fields through the entirety of the star-

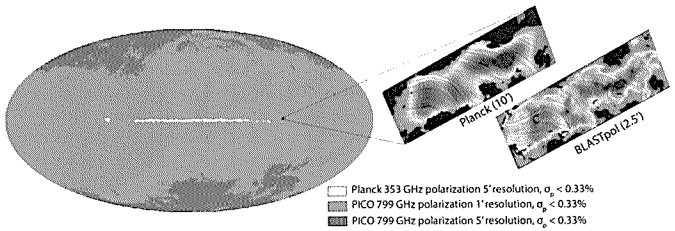

Figure 11: At 799 GHz, the PICO Baseline mission will map nearly the entire sky at $1'$ resolution with a sensitivity of 0.33% (The CBE will improve this to the entire sky at $1'$, $\sigma_p < 0.33\%$). As an example of the current state of the art, Planck ($10'$) and BLASTpol ($2.5'$) maps of the Vela C region are shown [90]. These observations will enable PICO to characterize magnetized turbulence from the diffuse ISM down to dense star-forming cores.

formation process.

Dust Physics

Strong extinction features at 9.7 and 18 μm indicate much interstellar dust is in the form of amorphous silicates, while features at 2175 Å, 3.3 μm, and 3.4 μm attest to abundant hydrocarbons. It is unknown, however, whether the silicate and carbonaceous materials coexist in the same grains or whether they are segregated into distinct grain populations. If there are indeed multiple grain species, this will induce additional challenges for modeling the emission from interstellar dust in both total intensity and polarization at levels relevant for B-mode science [91].

Spectropolarimetry of dust extinction features reveals robust polarization in the 9.7-μm silicate feature [e.g., 92], indicating that the silicate grains are aligned with the interstellar magnetic field. In contrast, searches for polarization in the 3.4-μm carbonaceous feature have yielded only upper limits, even along sightlines where silicate polarization is observed [93, 94]. These data suggest that most of the silicate and carbonaceous materials do not exist in the same grains. However, these studies are limited to only a few highly-extincted sightlines that may not typify the diffuse ISM.

At odds with the spectropolarimetric evidence from dust extinction, current measurements of the polarization fraction of the far-infrared dust emission with *Planck* [95] and BLASTPol [96] betray little to no frequency dependence, as would be expected if two components with distinct polarization properties were contributing to the total emission. However, current uncertainties are relatively large and the data with $\nu > 353$ GHz are from high-density sightlines that may not be representative of the diffuse ISM. With great polarization sensitivity even in diffuse regions, PICO will provide a definitive test of the two-component paradigm.

To assess PICO's ability to discriminate quantitatively, we employ the analytic two-component dust mode of [97], which provides a better fit to IRAS and *Planck* data than one-component models. Applying the noise estimates from PICO, 1000 simulations were run for different combinations of polarization fractions of the two components in this model. Only frequency channels 107 GHz and above were used, and the simulated data were binned to the 7.9′ beam of the PICO 107-GHz channel. Based on the variance of the simulation results, PICO can determine the intrinsic po-

larization fractions of the two components to a precision of 2%. PICO will therefore be able to validate or reject state-of-the-art dust models (e.g. [98, Hensley & Draine, in prep]) and test for the presence of additional grain species with distinct polarization signatures, such as magnetic nanoparticles [99].

Are Magnetic Fields Responsible For Low Star-Formation Efficiency?

Stars form out of dense, gravitationally unstable regions within molecular gas clouds. The efficiency of this conversion from molecular gas to stars is very low, due to regulation from supersonic turbulent gas motions, magnetic fields, and feedback from young stars [100]. Magnetic fields may play an important role in slowing the process of star formation by inhibiting movement of gas in the direction perpendicular to the field lines. Observations to date suggest that the outer envelopes of clouds can be supported against gravity by magnetic fields, but in dense cores gravity tends to dominate, and so these dense structures can collapse to form stars [101].

On larger scales, the formation of gravitationally unstable clouds is regulated by the flow of diffuse material into the molecular phase, a process that is mediated by magnetized turbulence in the low-density ISM. Structure formation in the diffuse ISM is poorly understood, but as a precursor to star formation it is crucial to understand what drives molecular-cloud formation. Recent observations suggest that the structure of the diffuse medium is highly anisotropic, and strongly coupled to the local magnetic field [102–105].

However, the degree to which magnetic fields affect the formation of molecular clouds, as well as stars within these clouds, is poorly constrained, in large part due to the difficulty of making detailed maps of magnetic fields in the interstellar medium.

• **Formation of Stars within Magnetized Molecular Clouds** With full-sky coverage and a best resolution of $1.1'$, PICO will be able to map all molecular clouds with better than 1-pc resolution, out to a distance of 3.4 kpc. Extrapolating from the Bolocam Galactic Plane Survey [BGPS, 106], PICO is expected to make highly detailed magnetic field maps of over 2,000 molecular clouds, with thousands to hundreds of thousands of independent measurements per cloud.

Our goal is to constrain both the strength of the magnetic field, B, within these clouds, as well as the energetic importance of the field compared to self-gravity (parameterized by the mass-to-flux ratio μ) and turbulence (parameterized by the Alfvén Mach number $\mathcal{M}$) as a function of density. To measure these quantities we will apply a series of established polarization analysis techniques: (1) characterizing the relative orientation of cloud structures and the magnetic field [107–110]; (2) making probability distributions functions of polarization measurables [90, 111]; (3) comparing between the magnetic field and velocity gradient directions [112–114]; and (4) measuring the angular dispersion of the magnetic field [115–118]. By applying all four techniques to both PICO observations and synthetic polarization maps made from "observing" numerical simulations of star formation, we will quantitatively compare theory and observations. PICO's large number of frequency bands will be used to better model the temperature and polarization efficiency of the cloud dust [119], which can then be used to generate more realistic synthetic observations from simulations, for comparison with PICO observations [120]. We can then compare the observed magnetization levels derived from the PICO observations to the levels of turbulence derived from molecular gas surveys (e.g.: Ellsworth-Bowers et al. 106, Miville-Deschênes et al. 121), and the efficiency of star formation, measured from near and far-IR observations of dense cores and protostars with *Herschel*, *Spitzer*, and *WISE*.

PICO's ability to map thousands of clouds is not possible with any other current or proposed